Pakistan Veterinary Journal

ISSN: 0253-8318 (PRINT), 2074-7764 (ONLINE)
DOI: 10.29261/pakvetj/2024.225

RESEARCH ARTICLE

Protective Effect of Lentinan against LPS-Induced Injury in Mice Via Influencing Antioxidant Enzyme Activity, Inflammatory Pathways and Gut Microbiota

Anqi Meng[1,2], Xiaojuan Zhang[3], Panduo Pubu[3], Munwar Ali[1,2], Jia Wang[1,2], Chang Xu[1, 2], Mikhlid H. Almutairi[4] and Kun Li[1,2*]

[1]Institute of Traditional Chinese Veterinary Medicine, College of Veterinary Medicine, Nanjing Agricultural University, Nanjing 210095 and PR China
[2]MOE Joint International Research Laboratory of Animal Health and Food Safety, College of Veterinary Medicine, Nanjing Agricultural University, Nanjing 210095, PR China
[3]Agriculture and Animal husbandry science and technology service station in Seni district, Naqu, 852000
[4]Zoology Department, College of Science, King Saud University, P.O. Box: 2455, 11451, Riyadh, Saudi Arabia
*Corresponding author: lk3005@njau.edu.cn

ARTICLE HISTORY (24-312)

Received:	June 8, 2024
Revised:	July 26, 2024
Accepted:	July 30, 2024
Published online:	August 08, 2024

Key words:
Lentinan
LPS
Antioxidant
anti-inflammatory
gut microbiota
mice

A B S T R A C T

Irrational use of antibiotics against Gram-negative bacteria results not only in gut dysbiosis but also leads to antimicrobial resistance (AMR). Consequently, natural products are being considered as an alternative to antibiotics. One such product is Lentinan (LNT), a polysaccharide found in edible mushroom, *Lentinula edodes*. This study was performed to evaluate the effects of LNT on overall intestinal health and gut microbiota in mice exposed to LPS. In this study, 30 male ICR mice were randomly divided into Control (C), Model (M), and Prophylactic (P) groups. For 13 days, groups C and M received a basal diet + normal saline, while group P received a basal diet + LNT (200 mg/kg of BW). Then groups M and P were exposed to LPS intraperitoneal injection (IP) (10 mg/kg) for 9 hours, and all mice were sacrificed for analysis on day 14th. LNT treatment significantly increased levels of glutathione peroxidase (GSH:Px) ($P<0.05$), interleukin-10 (IL-10) ($P<0.0001$), increased villi height ($P<0.0001$), the crypt depth ($P<0.001$), and beneficially modulated the relative abundance of bacteria, especially phylum Firmicutes, Bacteroidetes, Actinobacteria and genus *Campylobacter*. Other genera *Duncaniella* ($P<0.001$), *CAG-269* ($P<0.05$), and *Tidjanibacter* ($P<0.05$) were increased, while *Phocaeicola_A_858004* ($P<0.05$), *Enterococcus* ($P<0.0001$) and *D16-34* ($P<0.05$) were decreased after LNT supplementation. Altogether, LNT treatment improved antioxidant enzyme activity, intestinal integrity, and immune response, reduced inflammation, and induced a beneficial shift in gut microbiota to mitigate LPS-induced sepsis.

To Cite This Article: Meng A, Zhang X, Pubu P, Ali M, Wang J, Xu C, Almutairi MH and Li K, 2024. Protective effect of lentinan against LPS-induced injury in mice via influencing antioxidant enzyme activity, inflammatory pathways, and gut microbiota. Pak Vet J, 44(3): 647-656. http://dx.doi.org/10.29261/pakvetj/2024.225

INTRODUCTION

An impaired intestinal epithelial barrier can lead to the invasion of a variety of notorious pathogens and promote the occurrence of intestinal and systemic infections (Turner, 2009). Consequently, antibiotics are being used to cope with different types of infections. However, the irrational use of antibiotics has recently led to the emergence of antibiotic-resistant Gram-negative bacteria e.g. Salmonella and Escherichia coli (Xu *et al.*, 2017; Scott *et al.*, 2018). Lipopolysaccharide (LPS) being a key constituent of the cell wall in Gram-negative bacteria induces sepsis-like illness, leading to the activation of the innate immune system and promoting the secretion of inflammatory cytokines (Wang *et al.*, 2022). Gut dysbiosis in mice due to LPS has also been reported (Tang *et al.*, 2021). Consequently, there is a growing interest in anti-LPS dietary immunostimulants and the development of new antimicrobial strategies to address this ever-growing challenge.

One such immunostimulant with promising potential is LNT, a bioactive polysaccharide found in shiitake mushrooms. LNT (β-glucan) has antioxidant, anti-cancer, hypoglycemic, hypolipidemic and immunomodulatory properties (Meng *et al.*, 2020; Sheng *et al.*, 2021). LNT regulates the immune response by blocking toll-like

receptor 4 (TLR4), activating nuclear factor kappa B (NFκB), and decreasing the expression of interleukin-6 (IL-6), tumor necrosis factor-alpha (TNF-α), interleukin-1 beta (IL-1β) (Tsukamoto *et al.*, 2018; Liu *et al.*, 2019), and the activity of OX40/IL-17A signaling and stimulating the activation of nuclear factor erythroid 2 related factor (Nrf2), which is crucial in oxidative stress (Yang *et al.*, 2022b).

Recent studies have demonstrated LNT's ability to modulate intestinal microbiota composition and metabolites, thereby influencing host immune responses and protecting against intestinal injury induced by LPS. These findings suggest that lentinan holds promise as a therapeutic agent for mitigating the negative effects of Gram-negative bacterial infections, including their inflammatory and intestinal injury-inducing properties (Nishitani *et al.*, 2013; Xu and Zhang, 2015; Wang *et al.*, 2019a). Therefore, by clarifying its therapeutic potential, we can discover new methods to fight against Gram-negative bacteria.

MATERIALS AND METHODS

Experimental design: Thirty male ICR mice (n=30) weighing 20 ± 3 g each, were obtained from Nanjing Qinglongshan Animal Farm after approval of the ethical committee (NJAU.No.20230413054). The mice were kept at 25±2℃, with 12 hours in each cycle of dark and light periods, provided with free access to water and feed. The mice were arbitrarily divided into control (C), model (M) and prophylactic (P) groups. From day 1 to day 13, groups C and M were provided with a basal diet + saline solution of 0.01 mL/g of BW. On the other hand, group P received a basal diet + LNT at the dose of 200 mg/kg of BW (LNT was purchased from Shanghai Acmec Biochemical Technology Co., Ltd). After 13 days, mice in groups M and P were injected with an IP injection of LPS at the dose of 10 mg/kg of BW (LPS was delivered by Solarbio Life Science Co., LTD (Beijing, China). Following a 9-hour LPS exposure, all mice were euthanized. Blood, jejunal samples and rectal contents were taken from each mouse and promptly preserved at -80℃ for further analysis (Fig. 1).

Estimation of antioxidant enzyme activity and inflammatory cytokines: Mouse IL-10 ELISA kit (manufactured by Shanghai Jianglai Biotechnology Co., Ltd), malondialdehyde (MDA) test kit, glutathione peroxidase (GSH:Px) test kit, and total antioxidant capacity (T-AOC) kit (manufactured by Nanjing Jiancheng Institute of Bioengineering, China) were used to estimate the concentration of antioxidant enzymes and IL-10.

Histopathological analysis: The representative jejunal segments from each mouse were collected and fixed in 4% paraformaldehyde for 48 hours. The tissue samples were subsequently embedded in paraffin, sectioned to a thickness of 4-5μm, and stained with hematoxylin and eosin (H&E) for histopathological examination.

Genomic DNA extraction: OMEGA Soil DNA Kit (Omega Bio-Tek, Norcross, GA, USA) was used for total DNA extraction followed by measuring the amount of collected DNAs through a NanoDrop NC2000 spectrophotometer. The collected DNA was quality-tested by running an aliquot on 0.8% agarose gel.

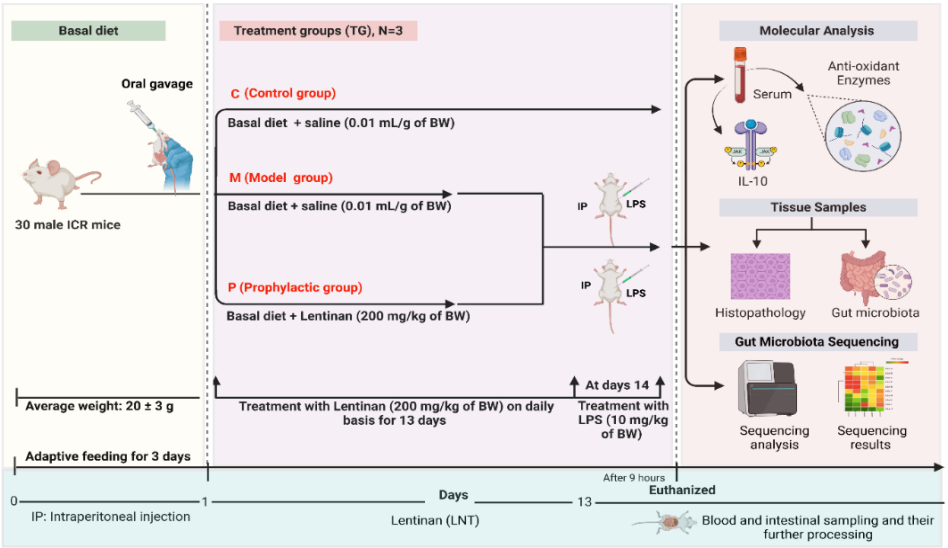

Fig. 1: Experimental design in the current study

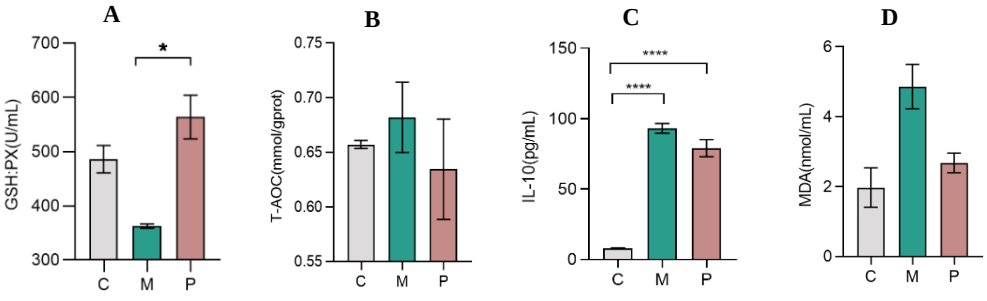

Fig. 2: Antioxidant and anti-inflammatory effects of LNT. (A) MDA, (B) GSH:Px, (C) T-AOC, and (D) IL-10. Significance is presented as *P<0.05, ***P<0.001, and ****P<0.0001; data were presented as the mean±SEM (n = 3).

16S rDNA gene amplification and sequencing: The V3–V4 regions of bacterial 16S rRNA genes were amplified using PCR with forward primer 338F and reverse primer 806R. Seven-base pair barcodes were incorporated to enable multiplex sequencing. Both primers were labeled with Illumina adapter and adapter sequences (Lundberg *et al.,* 2013). The PCR reaction mixture for each amplification reaction consisted of 12.5µL PCR Mix, 1.0µL DNA, 1.0µL each forward and reverse primers and 9.5µL high-pressure distilled water, with a total reaction volume of 25µL. PCR amplification was consisting a total of 35 PCR cycles, with each cycle having an initial hot start pre-denaturation temperature of 95℃ (5m); The denaturation temperature is 95℃(15 s); The primer annealing temperature Tm was 50℃(15s); Elongation at 72℃ (45s); Then the final extension at 72℃ (10 m); Finally, stored at 4℃.

To remove non-specific products, purification of PCR amplicons was performed using Vazyme VAHTSTM DNA Clean Beads. Purified PCR amplifications were used to prepare libraries in the Illumina TruSeq Nano DNA LT Library Prep Kit following the manufacturer's recommendations. The quality of the resultant library was then detected through Quant-iT PicoGreen dsDNA Assay Kit. Finally, 2×250 bp paired-end sequencing was conducted for qualified libraries for high-throughput sequencing on Illumina platforms with MiSeq Reagent Kit v3.

Bioinformatics analysis: Raw sequences obtained after high-throughput sequencing were subjected to pre-processing using the DADA2 method in QIIME2 (version 2023.7). This pre-processing involved filtering, dereplication, chimera identification and merging of paired-end reads. The resulting (Callahan *et al.,* 2016), high-quality sequences obtained were classified into the same operational amplicon sequence variants (ASVs) or taxonomic unit (OTU) based on a 95% similarity threshold. To assess the present level of sequencing depth rarefaction curve was plotted. The alpha-diversities were computed using the abundance of ASVs or OTUs, (observed_OTUs, Chao1, faith_pd and Shannon indexes) and beta diversities using PCoA plots and UPGMA. The QIIME2 program was utilized for diversity analysis. The LEfSe analysis was performed to compare the taxon with differential abundance between the groups.

Statistical analysis: The Kruskal-Wallis test, ANOVA, chi-square test, Dunn's test and software programs GraphPad Prism (v9.0) and SPSS (v26.0) were used considering $P<0.05$ as statistically significant.

RESULTS

Consequences of LNT therapy on antioxidant enzyme activity and inflammatory cytokines: Concentration of Malondialdehyde (MDA) was elevated in group M, but LNT decreased MDA in group P (Fig. 2A). The level of GSH:Px in group M was significantly lower ($P<0.05$) than group P (Fig. 2B). There was insignificant variation in the T-AOC across the three groups (Fig. 2C). The findings also demonstrated a considerably elevated level of IL-10 ($P<0.0001$) in group M but LNT treatment reduced IL-10 ($P<0.0001$) levels (Fig. 2D).

Histopathological observations: Histopathological analysis of the jejunum after H & E staining revealed significant differences among the groups. Compared to group C, group M displayed severe epithelial damage characterized by villus atrophy, blunting, and plasma cell infiltration in the lamina propria. In contrast, group P exhibited preserved epithelial integrity, with well-defined villus architecture, significantly increased villus height, and visible crypt structures (Fig. 3A). The villus height in group M was significantly shorter compared to group P ($P<0.0001$) (Fig. 3B). Both groups M and P showed increased jejunal crypt depth compared to group C, but the increase in crypt depth was less pronounced in group P than in group M ($P<0.001$) (Fig. 3C).

Sequencing data analysis: 16S rDNA and ITS amplicon sequencing resulted in a total of 418250, 416703, and 420588 raw sequences regarding groups C, M, and P, respectively with more than 91% filtered data in all groups, varying from 63548 to 90912 per sample (Table 1). Each de-emphasized sequence produced after noise reduction using DADA2 is termed ASV/OTU, and there were conserved microbial communities in varying environmental conditions up to a certain degree.

The gradual flattening of the Rarefaction Curve showed that the sequencing quantity and depth had covered all the species in the samples and satisfied the requirements of further study (Fig. 4A). To interpret species abundance and species evenness, OTU-abundance curves were constructed. Each fold line denotes a sample (group), and the length of the fold line on the horizontal axis indicates the number of ASVs/OTUs in that sample (group) at that abundance. A flatter fold line suggests a smaller variation in abundance among ASVs/OTUs within the community (Fig. 4B).

Gut microbial diversity analysis: Multiple α-diversity indices described the diversity and richness of microorganisms, indicating that the faith_pd in group M was less compared to group P and that Chao1, observed_features, and Shannon were higher compared to group P (Fig. 5A). Moreover, Shannon had a significant variation ($P<0.05$), which suggested that the sample microbiota of the mice in group P had better homogeneity and richness and poor diversity ($P>0.05$).

The β-diversity indices, such as Principal Coordinates Analysis (PCoA), provide a measure of the similarity in community composition among the samples (Fig. 4B). Analysis of the Jaccard distance revealed that the points in groups M and P were separated by a specific distance. This indicates that the gut microbial structure LNT-treated group changed following LPS induction (Fig. 5B). The NMDS statistics demonstrated the variations both among and within the samples (Fig. 5C). The UPGMA plots demonstrated that the similarity between the two samples increased as the branching length between them decreased (Fig. 5D). The PERMANOVA analysis revealed significant differences within groups and between groups (Fig. 5E).

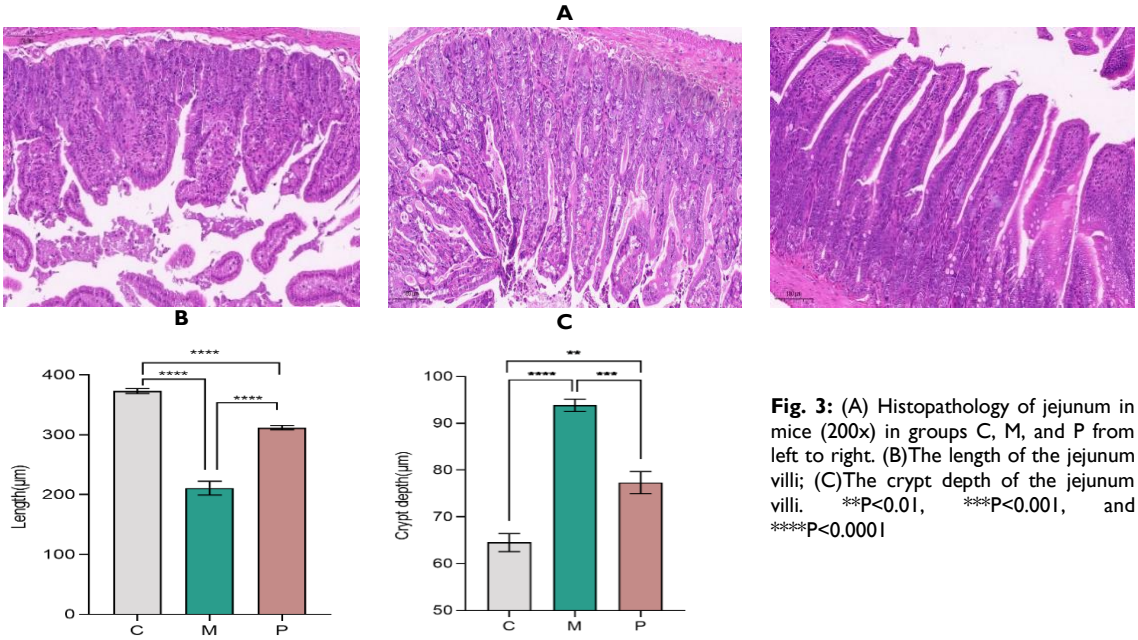

Fig. 3: (A) Histopathology of jejunum in mice (200x) in groups C, M, and P from left to right. (B)The length of the jejunum villi; (C)The crypt depth of the jejunum villi. **P<0.01, ***P<0.001, and ****P<0.0001

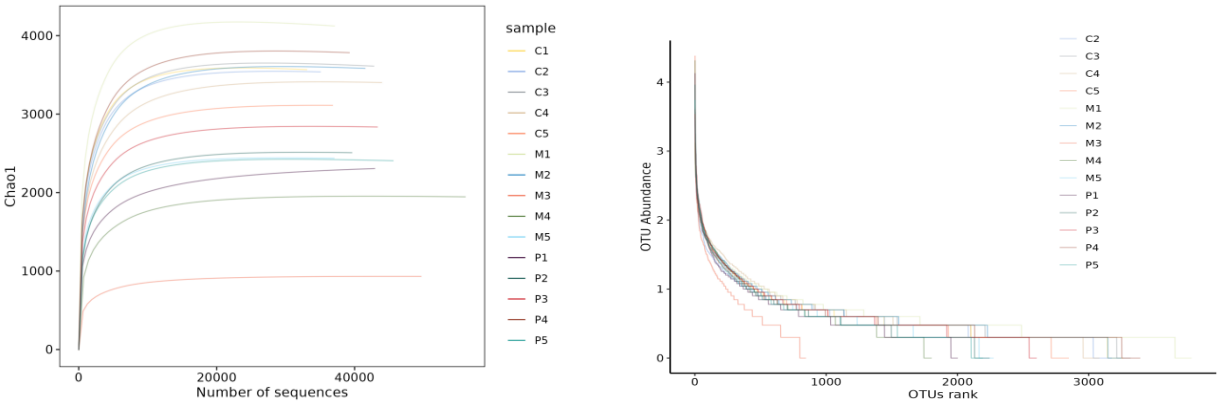

Fig. 4: Sequencing data analysis and OUT distribution, (A) Rarefaction Curve; (B) Rank abundance curve.

Gut microbial composition analysis: Phylum Firmicutes (C = 35.53%, M = 45.46%, P = 43.65%) and Bacteroidota (C = 57.35%, M = 44.99 %, P = 44.61%) were dominant being more than 88%. Actinobacteriota accounted for a higher proportion of 5.04% in group M, 3.46% and 3.57% in groups C and P, respectively, while Campylobacterota accounted for a lower proportion of 1.84% in group M and 2.55% and 6.79% in groups C and P, respectively. The percentage of Desulfobacterota_I increased in both group M and P, but the increase was greater in group M (C=0.59%, M=2.27%, P=1.17%), while Proteobacteria showed a trend of increasing in group M and decreasing in group P, compared to group C (C=0.27%, M=0.34%, P = 0.12%). At the genus level, Bacteroidia, Bacilli and Clostridia_258483 were the dominant organisms in the C, M and P groups, with proportions of C=57.35%, 22.58%, 12.88%; M=45.00%, 33.97%, 11.49% and P=44.61%, 27.37%, 16.27%.

For the top ten species ranked at the genus level, in group M, Lactobacillus, Limosilactobacillus, and Paramuribaculum dominated being 17.22%, 12.82% and 11.71%. Group P had Lactobacillus, Paramuribaculum, and Limosilactobacillus as the dominant flora being 19.22%, 8.23% and 7.86% respectively. Among them, the abundance of Lactobacillus, Prevotella, and Duncaniella was relatively high in group P compared to group M. Cryptobacteroides showed a decline in group M and an increase in group P (C=3.52%. M=2.11%, P=5.61%). These results indicated that LNT increased the abundance of species of Firmicutes, Clostridia, Cryptobacteroide, Lactobacillus, Prevotella, and Duncaniella and decreased the abundance of Bacteroidota, Actinobacteriota, Desulfobacterota_I, and Proteobacteria in the intestinal tracts of LPS treated mice.

Performing LEfSe (|LDA score|> 2.0) detected that Helicobacter_C_479931, Duncaniella, Rikenella, and Rikenellaceae in group C, while Phocaeicola_A_858004 in group M were more prevalent (Fig. 6E). Furthermore, group P exhibited the presence of two biomarkers, namely Parabacteroides_B_862066 and Tannerellaceae. The concentric rings in the cladistic graphic depict taxonomic ranks ranging from phylum to genus (or species) (Fig. 6E). In the MetaCyc pathway, there was one up-regulated differential metabolite in group C and one down-regulated differential metabolite in group P, with 10 up-regulated different differential metabolites in group M. In KEGG pathways, only group M has one upregulated differential metabolite, which is Steroid hormone biosynthesis (Fig. 6G).

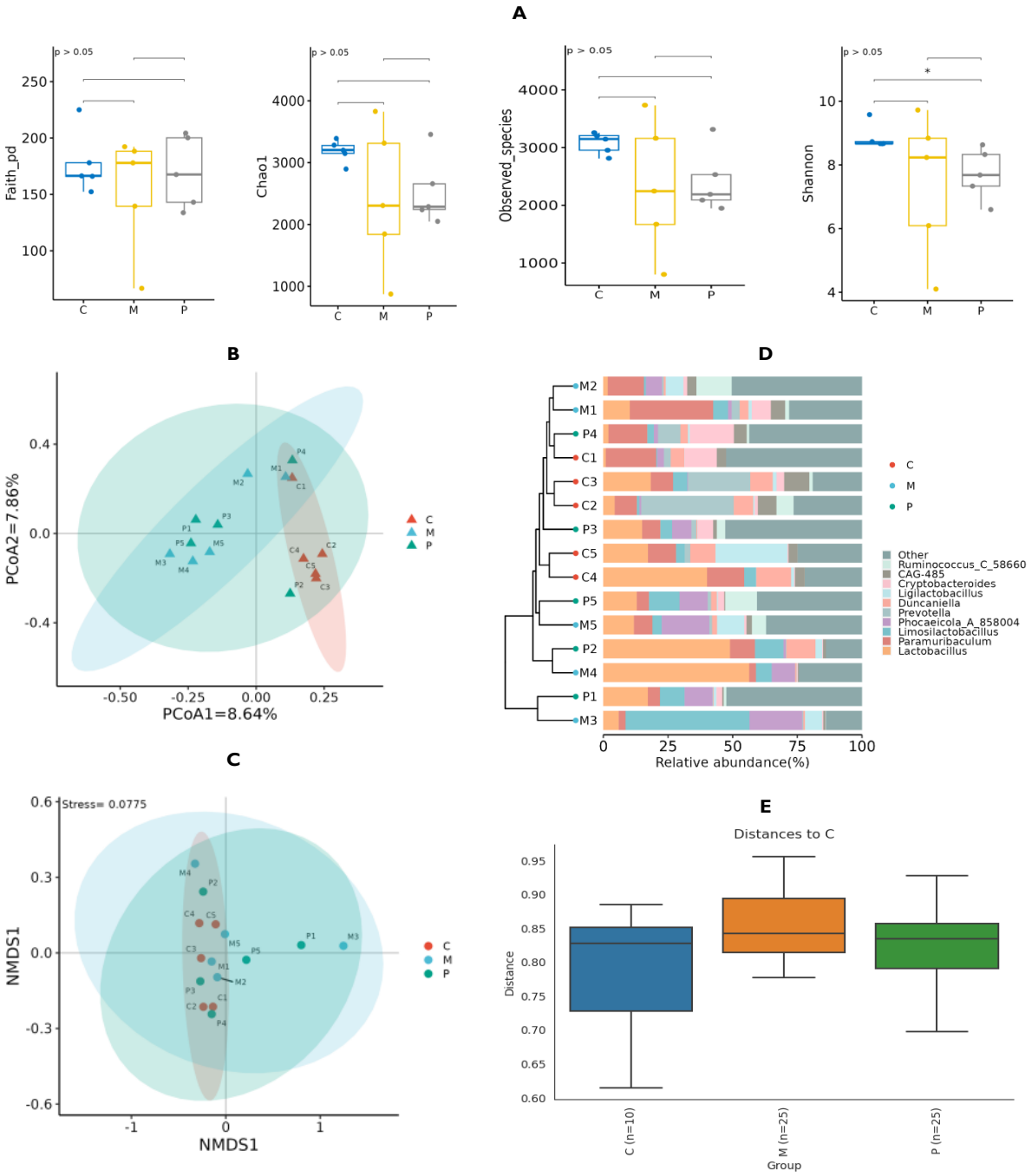

Fig. 5: (A) α-diversity indices: faith_pd, chao1, observed_OTUs, and Shannon. (B) PCoA plots based on the Jaccard distance. (C) NMDS. (D) Unweighted pair-group method with arithmetic means (E) PERMANOVA.

Table 1: The sequenced data of mice microbiome in the present study.

Sample ID	Input	Filtered	Percentage of input passed filter	Denoisd	Merged	Percentage of input merged	Non-chimeric	Percentage of input non-chimeric
C1	79376	73499	92.60	69584	49212	62.00	34661	43.67
C2	76379	71027	92.99	68460	51193	67.02	36218	47.42
C3	90124	83336	92.47	81278	65373	72.54	44121	48.96
C4	90613	83493	92.14	81369	67313	74.29	45047	49.71
C5	81758	74687	91.35	72317	57610	70.46	37792	46.22
M1	84322	77204	91.56	74443	56247	66.71	38711	45.91
M2	95257	88204	92.60	85197	66509	69.82	42921	45.06
M3	68486	63548	92.79	62839	59399	86.73	49807	72.73
M4	87542	81280	92.85	78909	68080	77.77	56539	64.58
M5	81096	75013	92.50	71573	54865	67.65	37703	46.49
P1	74027	69031	93.25	67183	57861	78.16	43659	58.98
P2	69955	64231	91.82	62873	53675	76.73	40424	57.79
P3	97892	90912	92.87	86722	66048	67.47	44131	45.08
P4	86781	80125	92.33	77711	60737	69.99	40917	47.15
P5	91933	85499	93.00	82686	69491	75.59	46239	50.30

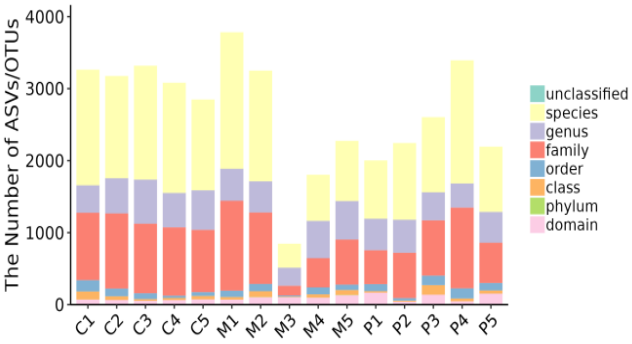
The Number of ASVs/OTUs
4000
3000
2000
1000
0
C1 C2 C3 C4 C5 M1 M2 M3 M4 M5 P1 P2 P3 P4 P5
unclassified
species
genus
family
order
class
phylum
domain

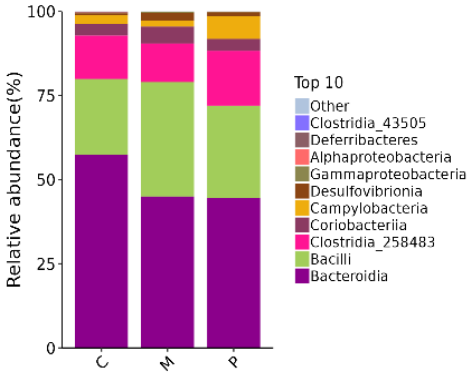
Relative abundance(%)
100
75
50
25
0
C M P
Top 10
Other
Clostridia_43505
Deferribacteres
Alphaproteobacteria
Gammaproteobacteria
Desulfovibrionia
Campylobacteria
Coriobacteriia
Clostridia_258483
Bacilli
Bacteroidia

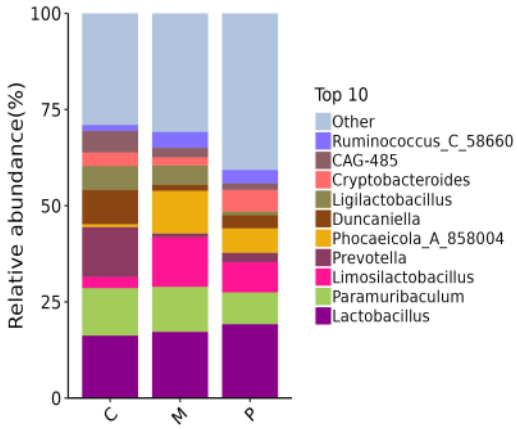
Relative abundance(%)
100
75
50
25
0
C M P
Top 10
Other
Ruminococcus_C_58660
CAG-485
Cryptobacteroides
Ligilactobacillus
Duncaniella
Phocaeicola_A_858004
Prevotella
Limosilactobacillus
Paramuribaculum
Lactobacillus

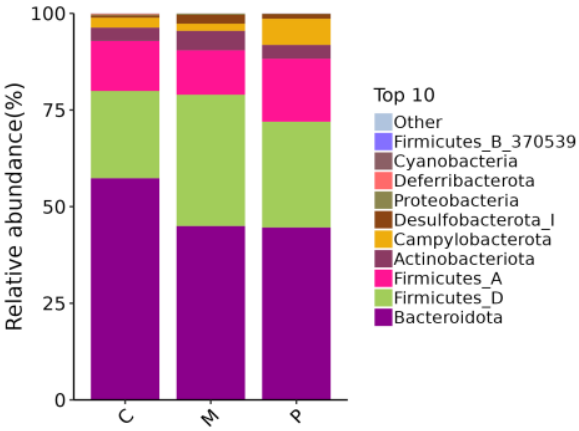
Relative abundance(%)
100
75
50
25
0
C M P
Top 10
Other
Firmicutes_B_370539
Cyanobacteria
Deferribacterota
Proteobacteria
Desulfobacterota_I
Campylobacterota
Actinobacteriota
Firmicutes_A
Firmicutes_D
Bacteroidota

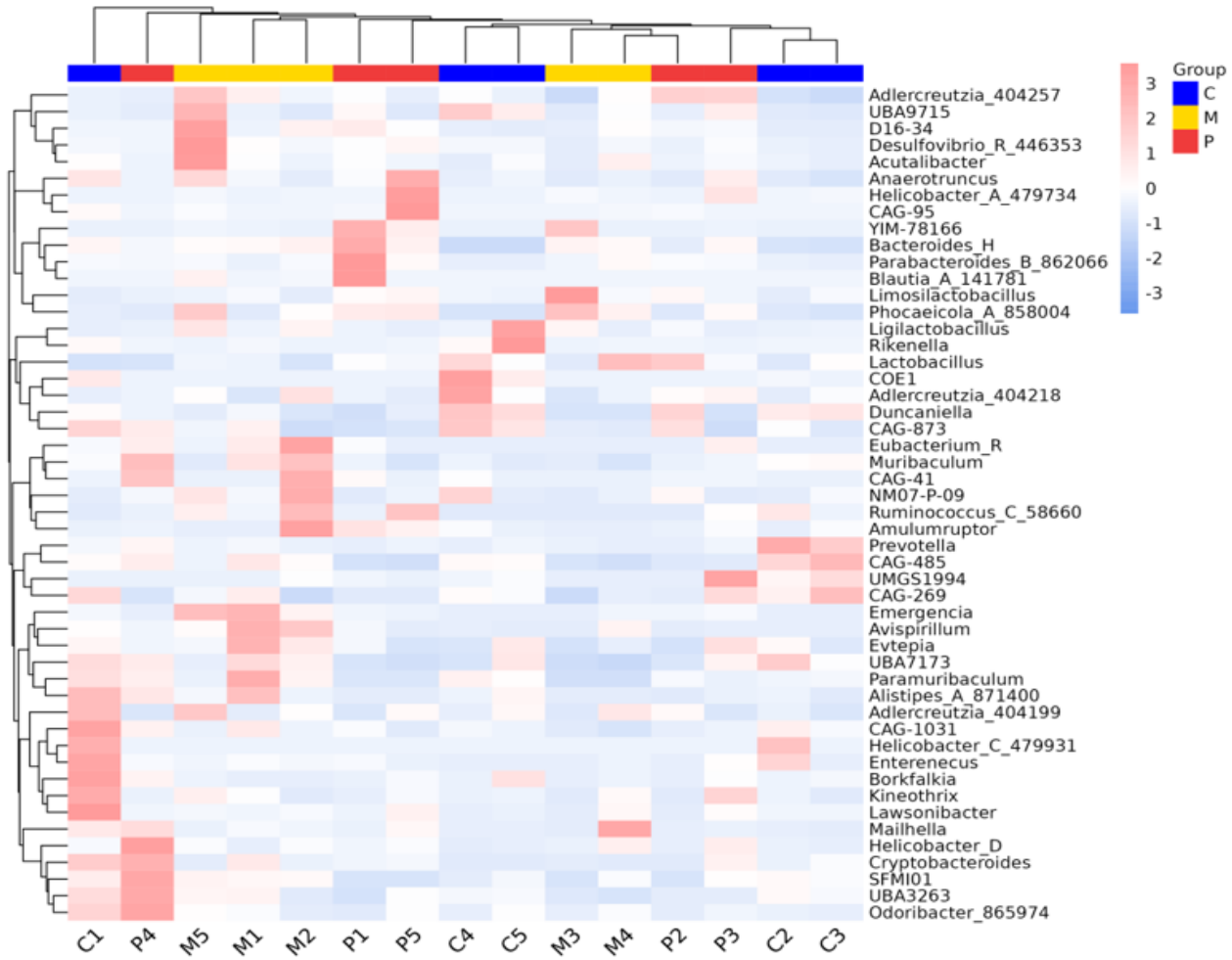
Group
C
M
P
3
2
1
0
-1
-2
-3
Adlercreutzia_404257
UBA9715
D16-34
Desulfovibrio_R_446353
Acutalibacter
Anaerotruncus
Helicobacter_A_479734
CAG-95
YIM-78166
Bacteroides_H
Parabacteroides_B_862066
Blautia_A_141781
Limosilactobacillus
Phocaeicola_A_858004
Ligilactobacillus
Rikenella
Lactobacillus
COE1
Adlercreutzia_404218
Duncaniella
CAG-873
Eubacterium_R
Muribaculum
CAG-41
NM07-P-09
Ruminococcus_C_58660
Amulumruptor
Prevotella
CAG-485
UMGS1994
CAG-269
Emergencia
Avispirillum
Evtepia
UBA7173
Paramuribaculum
Alistipes_A_871400
Adlercreutzia_404199
CAG-1031
Helicobacter_C_479931
Enterenecus
Borkfalkia
Kineothrix
Lawsonibacter
Mailhella
Helicobacter_D
Cryptobacteroides
SFMI01
UBA3263
Odoribacter_865974
C1 P4 M5 M1 M2 P1 P5 C4 C5 M3 M4 P2 P3 C2 C3

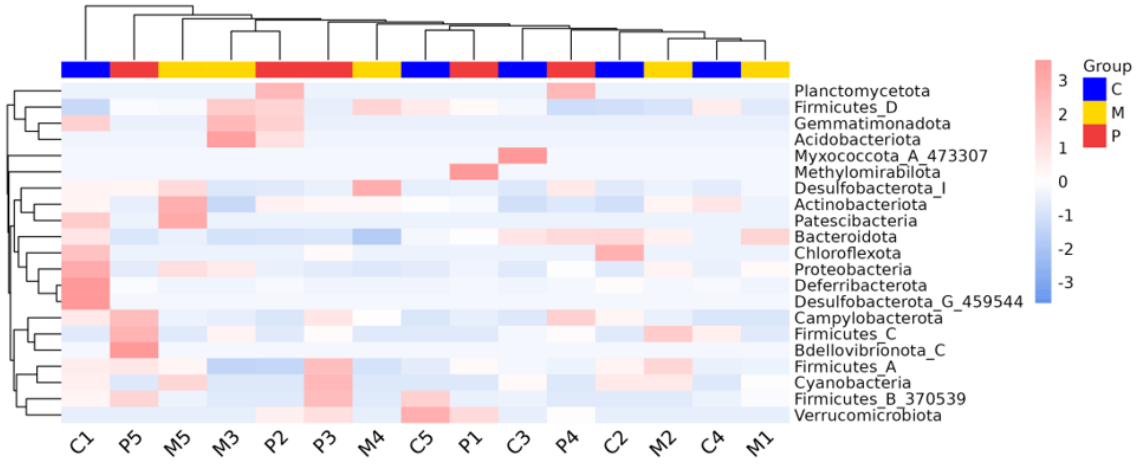
Group
C
M
P
3
2
1
0
-1
-2
-3
Planctomycetota
Firmicutes_D
Gemmatimonadota
Acidobacteriota
Myxococcota_A_473307
Methylomirabilota
Desulfobacterota_I
Actinobacteriota
Patescibacteria
Bacteroidota
Chloroflexota
Proteobacteria
Deferribacterota
Desulfobacterota_G_459544
Campylobacterota
Firmicutes_C
Bdellovibrionota_C
Firmicutes_A
Cyanobacteria
Firmicutes_B_370539
Verrucomicrobiota
C1 P5 M5 M3 P2 P3 M4 C5 P1 C3 P4 C2 M2 C4 M1

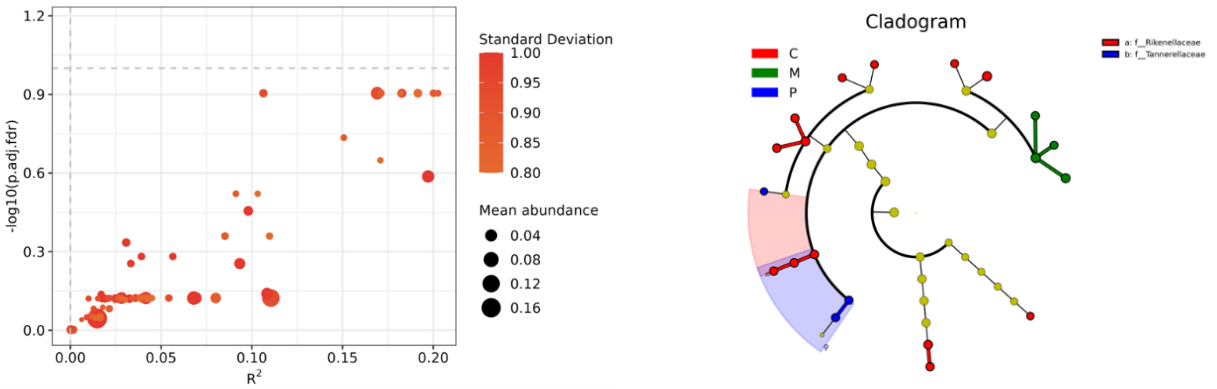
-log10(p.adj.fdr)
R²
Standard Deviation
1.00
0.95
0.90
0.85
0.80
Mean abundance
0.04
0.08
0.12
0.16
Cladogram
C
M
P
a: f__Rikenellaceae
b: f__Tannerellaceae

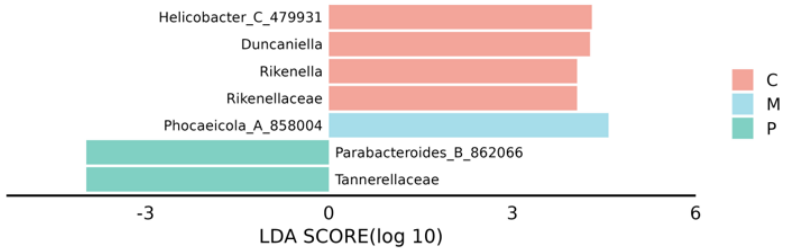
Helicobacter_C_479931
Duncaniella
Rikenella
Rikenellaceae
Phocaeicola_A_858004
Parabacteroides_B_862066
Tannerellaceae
C
M
P
LDA SCORE(log 10)

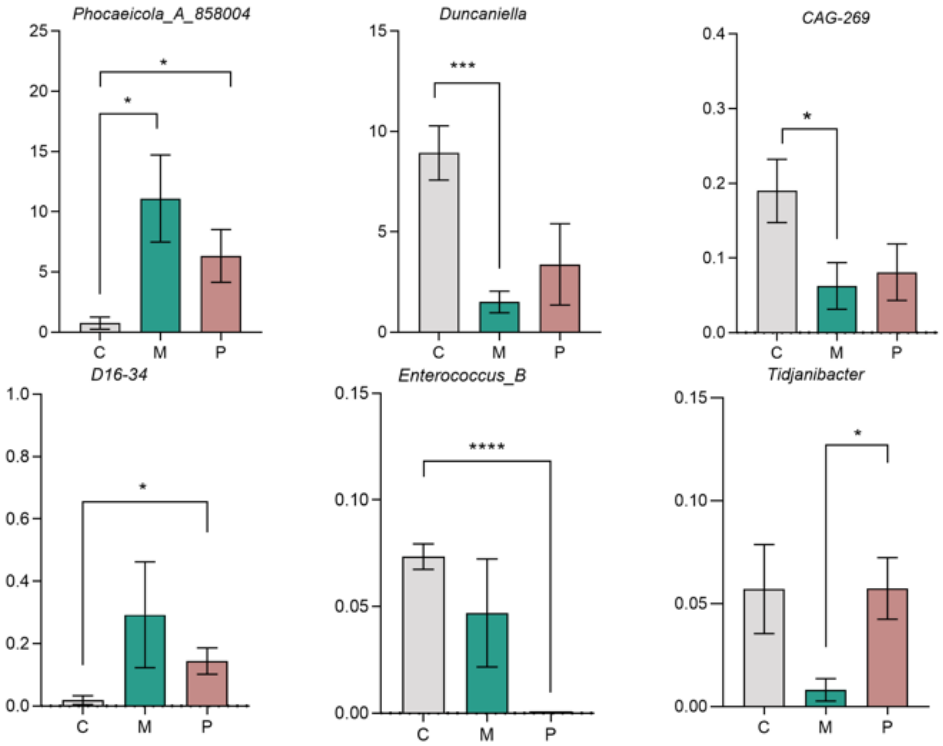
Phocaeicola_A_858004
Duncaniella
CAG-269
D16-34
Enterococcus_B
Tidjanibacter
C M P

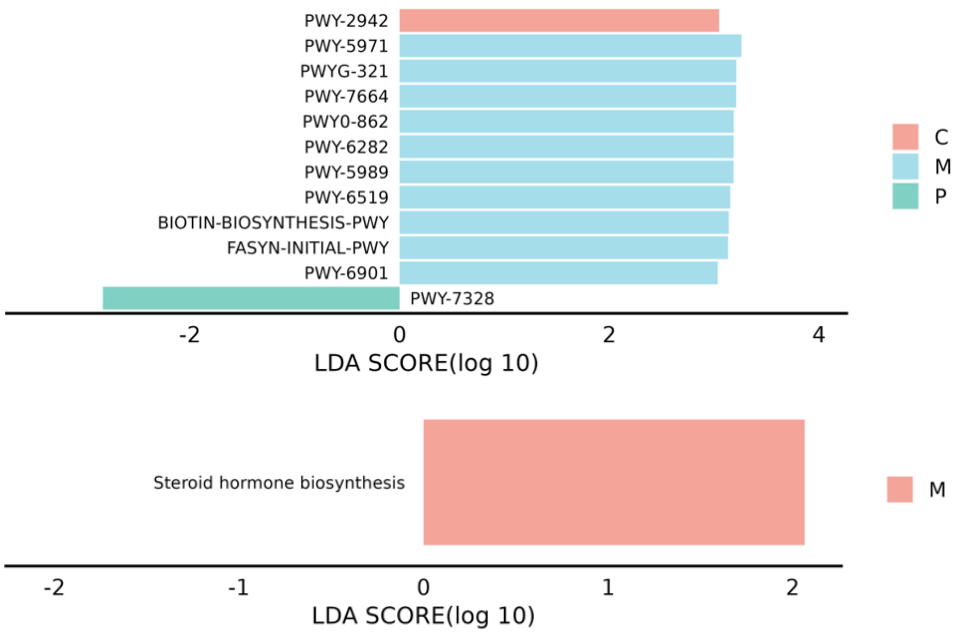

Fig. 6: (A) Statistical analysis of ASVs in different taxonomic units, (B) The dominant bacteria at phylum, class, and genus level; (C) heat map of bacterial distribution at phylum and genus level. (D) ZicoSeq analysis of ASVs; (E) LEfSe analysis: |LDA score| > 2.0 was considered as a significant difference, (F) Microbiota with significant differences at the genus level. (G) Distinguished pathways in MetaCyc pathways and KEGG pathways.

DISCUSSION

LNT exhibits diverse biological activities and has a positive safety profile (Ren *et al.*, 2015; Meng *et al.*, 2020; Sheng *et al.*, 2021). LNT enhances the integrity of the intestinal barrier by improving its antioxidant capacity (Wang *et al.*, 2019b; Huang *et al.*, 2022; Qin *et al.*, 2022). The administration of LNT reduced oxidative damage by reducing the levels of MDA and boosting the activity of GSH:Px (Fig. 2A, B). Ren *et al.* (2019) also discovered a notable increase ($P < 0.05$) in the activities of SOD, GSH:Px, CAT and MDA following LNT therapy in Hucho taimen. In the current study, IL-10 significantly reduced ($P<0.0001$) in the LPS-induced-LNT-treated group (Fig. 2D). This finding is in accordance with the report by Li *et al.* (2023). We investigated that LNT significantly enhanced the villus length ($P<0.001$) and reduced crypt depth ($P<0.001$), particularly in the jejunum and reduced inflammation (Fig. 3A). Ren *et al.* (2019) also demonstrated comparable findings. LNT in the intestine blocks the NF-κB signaling pathway and reduces the levels of TNF-α, IL-6, IL-1β, and IL-8 (Ren *et al.*, 2016; Ren *et al.*, 2019). Previous results also demonstrated that administering LNT orally at a dosage of 10 mg/kg led to a reduction in IL-10 levels in rabbits (Alkenany and Khalil, 2022). For its anti-inflammatory properties, LNT functions by mitigating the excessive inflammatory response of the body (Zhou *et al.*, 2024).

The analysis of alpha (Fig. 5 A) and beta-diversity indices (Fig. 5 B, C, D, E) revealed substantial differences ($P>0.05$) in the microbiota composition among all groups. The predominant taxa were Firmicutes (41.55% ± 3.74%) and Bacteroidota (48.98% ± 5.12%). Contrarily, Ren *et al.* (2016) found that LNT reduced Firmicutes and raised Bacteroidetes. One possible explanation for this variance could be that they evaluated the caecum concerning bacterial fermentation, rather than the jejunum. In our study, Phylum Bacteroidetes, specifically, the Phocaeicola, was seen to significantly decrease ($P<0.05$) in the P group compared to the M group (Fig. 6 E). This could perhaps be a compensatory mechanism to alleviate the detrimental impact of LPS in group M. Bacteroidetes produce short-chain fatty acids (SCFAs) and significantly affect carbohydrate fermentation, nitrogen use and pathogen decolonization (Xu *et al.*, 2012; Zhang *et al.*, 2016). After LNT treatment, a significant rise ($P<0.05$) in the abundance of CAG-269 (Firmicutes) was observed in the current study. Recent research emphasizes the importance of CAG-269 in inflammatory bowel disease (IBD) and colorectal cancer (CRC) (Minot and Willis, 2019). Furthermore, D16-34 were elevated in the treated group and decreased significantly ($P<0.05$) in LNT treated group. Furthermore, it was observed that the genus Tidjanibacter exhibited a significant increase ($P<0.05$) following LNT treatment (Fig. 6F). Research conducted by Rodas *et al.*, (2024) has shown that this genus plays a significant role in intestinal fermentation. The abundance of Enterococcus was dramatically reduced ($P<0.0001$) following LNT therapy (Fig. 6F). However, contrasting findings were reported by Yang *et al.* (2022a). Possible factors contributing to this variation include variations in the concentration of LNT and differences in the breed of mice used. Enterococcus functions as a commensal bacterium and has probiotic properties (Pont *et al.*, 2024). We investigated that Bacteroidia, Bacilli and Clostridia_258483 were the most prevalent in the P groups, accounting for 44.61%, 27.37% and 16.27% respectively (Fig. 6B). Clostridia plays a positive role in energy metabolism and contributes to the production of SCFAs (Lopetuso *et al.*, 2013).

The percentages of Lactobacillus, Paramuribaculum, and Limosilactobacillus in the P group were 19.22%, 8.23% and 7.86%, respectively. Group P exhibited a relatively high abundance of Lactobacillus, Prevotella and Duncaniella compared to group M (Fig. 6B) and Lirong *et al.* (2023) discovered similar patterns. Proteobacteria increased in group M and decreased in group P (C=0.27%, M=0.34%, P=0.12%) (Fig. 6 B, C) (Chu *et al.*, 2023). Proteobacteria, particularly Enterobacteriaceae are responsible for intestinal dysbiosis, influencing the anti-inflammatory response (Schippa and Conte, 2014; Ren *et*

al., 2019). A similar type of gut microbiota variation was observed by Lei *et al.* (2023), in a pig model infected with *Cryptosporidium*.

Thus, LNT hindered dysbiosis by reducing the abundance of Proteobacteria (Yang *et al.*, 2022a). Actinobacteriota constituted a greater percentage of 5.04% in group M, in contrast to groups C and P, which had proportions of 3.46% and 3.57% compatibly (Fig. 6 B, C). Actinobacteria (Bifidobacterium) have been identified as probiotics that enhance lipid metabolism (Yang *et al.*, 2022a). The prevalence of Campylobacterota was 2.55% in group C and 6.79% in group P (Fig. 6 B, C). The bile adaption of Campylobacter jejuni is linked to flagellins and 19 other proteins (Army *et al.*, 2023). Group P exhibited a notable upward trend of 5.61% in Cryptobacteroides (Fig. 6 B, C). Furthermore, the clustering heat map demonstrated that LNT increased the presence of Firmicutes, Clostridia, Cryptobacteroide, Lactobacillus, Prevotella, and Duncaniella species, while decreasing the abundance of Bacteroidota, Actinobacteriota, Desulfobacterota_I and Proteobacteria in the intestinal tracts of mice with LPS-induced inflammation (Fig. 6 B, C) (Yin *et al.*, 2023; Yanling *et al.*, 2023).

LNT increased the abundance of Prevotella (Fig. 6B). Prevotella also plays a crucial role in breaking down fiber and production of SCFAs (Kobayashi *et al.*, 2017). Therefore, the addition of LNT has a potential impact on preserving the health of the gut by preventing inflammation and oxidative harm, promoting the formation of SCFAs and modifying the makeup of the microbiota (Tang *et al.*, 2018).

Conclusions: In conclusion, LNT significantly improved antioxidant enzymes, and intestinal histopathology, particularly in the jejunum, acts as an anti-inflammatory compound by influencing different inflammatory pathways and cytokines (e.g. IL-10), modulated gut microbiota in a more beneficial way and has no toxicity for the host.

Ethical statement: The experiment with mice was conducted after approval of the Animal Welfare Committee of Nanjing Agricultural University on the Ethics of Animal Care (NJAU.No.20230413054).

Authors contributions: AM: writing – original draft, review, data curation, conceptualization. XJZ: reagents, materials, and analysis tools. PDPB: reagents, materials, and analysis tools. MA: writing – original draft, review, editing, data curation. KL: conceptualization, review, editing, validation and supervision. MHA: editing, data curation, proofreading. JW: writing. CX: editing. All authors know and approve the final manuscript.

Funding: The work was granted by the National Natural Science Foundation of China (32102692).

Conflicts of Interest: The authors declare no conflict of interest.

Acknowledgments: The authors extend their appreciation to the Researchers Supporting Project number (RSP2024R191), King Saud University, Riyadh, Saudi Arabia.

REFERENCES

Alkenany MR and Khalil LW, 2022. The effect of Lentinan administration on some immunological and biochemical parameters in intact rabbits. Int J Health Sci 6(3):6362-6381.

Army P, Mingyang W, Longbin W, *et al.*, 2023. Study on Bacterial Community in Fish Gut and Culture Environment in Racetrack Culture System of Seawater Pond. J Ocean Univ China (Nat Sci) 53: 47-60.

Callahan BJ, Mcmurdie PJ, Rosen MJ, *et al.*, 2016. DADA2: High-resolution sample inference from Illumina amplicon data. Nat Methods 13: 581-583.

Chu FY, Wang M, Li YJ, *et al.*, 2023. Effect of Auricularia auricula melanin on physiological indicators and intestinal flora in mice with iron deficiency anemia. Food Sci 44(5): 128-135.

Huang F, Shen X, Zhang Y, *et al.*, 2022. Postprandial changes of oxidative stress biomarkers in healthy individuals. Front Nutr 9: 1007304.

Kobayashi M, Mikami D, Kimura H, *et al.*, 2017. Short-chain fatty acids, GPR41 and GPR43 ligands, inhibit TNF-α-induced MCP-1 expression by modulating p38 and JNK signaling pathways in human renal cortical epithelial cells. Biochem Biophys Res Commun 486(2): 499-505.

Lei W, Sijia L, Wen Z, Sun N, *et al.*, 2023. The effects of Cryptosporidium infection on gut fungi and enzyme abundance in Sus domesticus. Asian J Agric Biol 2023(4): 2023114.

Li YL, Qin SY, Li Q, *et al.*, 2023. Jinzhen Oral Liquid alleviates lipopolysaccharide-induced acute lung injury through modulating TLR4/MyD88/NF-κB pathway. Phytomedicine114: 154744.

Lirong R, Yingrun F, Zelin L, *et al.*, 2023. Protective Effect of Tremella aurantialba Polysaccharide on Immunosuppressed Mice Induced by Cyclophosphamide. Food Res Dev 44.

Liu Y, Zhao J, Zhao Y, *et al.*, 2019. Therapeutic effects of lentinan on inflammatory bowel disease and colitis-associated cancer. J Cell Mol Med 23: 750-760.

Lopetuso L. R, Scaldaferri F, Petito V, *et al.*, 2013. Commensal Clostridia: leading players in the maintenance of gut homeostasis. Gut Pathog 23:1-8.

Lundberg D. S, Yourstone S, Mieczkowski P *et al.*, 2013. Practical innovations for high-throughput amplicon sequencing. Nat Methods 10: 999-1002.

Meng Y, Lyu F, Xu X, *et al.*, 2020. Recent advances in chain conformation and bioactivities of triple-helix polysaccharides. Biomacromolecules 21: 1653-1677.

Minot SS and Willis AD, 2019. Clustering co-abundant genes identifies components of the gut microbiome that are reproducibly associated with colorectal cancer and inflammatory bowel disease. Microbiome 7: 110.

Nishitani Y, Zhang L, Yoshida M, *et al.*, 2013. Intestinal anti-inflammatory activity of lentinan: influence on IL-8 and TNFR1 expression in intestinal epithelial cells. PloS One 22;8(4):e62441.

Pont CL, Bernay B, Gérard M, *et al.*, 2024. Proteomic characterization of persisters in Enterococcus faecium. BMC Microbiol 3: 24(1):9.

Qin S, She F, Zhao F, *et al.*, 2022. Selenium-chitosan alleviates the toxic effects of Zearalenone on antioxidant and immune function in mice. Front Vet Sci 6(9):1036104

Ren G, Li K, Hu Y, *et al.*, 2015. Optimization of selenizing conditions for Seleno-Lentinan and its characteristics. Int J Biol Macromol 81: 249-258.

Ren G, Xu L, Lu T, *et al.*, 2019. Protective effects of lentinan on lipopolysaccharide induced inflammatory response in intestine of juvenile taimen (Hucho taimen, Pallas). Int J Biol Macromol 121: 317-325.

Ren G, Yu M, Li K, *et al.*, 2016. Seleno-lentinan prevents chronic pancreatitis development and modulates gut microbiota in mice. J Funct Foods 22:177-188.

Rodas JA, Leon-rojas J and Rooney B, 2024. Mind over mood: exploring the executive function's role in downregulation. Front Psychol 25(15): 1322055.

Schippa S. and Conte MP, 2014. Dysbiotic events in gut microbiota: impact on human health. Nutrients 6: 5786-5805.

Scott NA, Andrusaite A, Andersen P, Lawson M, *et al.*, 2018. Antibiotics induce sustained dysregulation of intestinal T cell immunity by perturbing macrophage homeostasis. Sci Transl Med 10(464): eaao4755.

Sheng K, Wang C, Chen B, *et al.*, 2021. Recent advances in polysaccharides from Lentinus edodes (Berk.): Isolation, structures and bioactivities. Food Chem 358: 129883.

Tang J, Xu L, Zeng Y, *et al.*, 2021. Effect of gut microbiota on LPS-induced acute lung injury by regulating the TLR4/NF-kB signaling pathway. Int Immunopharmacol 91: 107272.

Tang R, Wei Y, Li Y, *et al.*, 2018. Gut microbial profile is altered in primary biliary cholangitis and partially restored after UDCA therapy. Gut microbiota 67: 534-541.

Tsukamoto H, Takeuchi S, Kubota K, *et al.*, 2018. Lipopolysaccharide (LPS)-binding protein stimulates CD14-dependent Toll-like receptor 4 internalization and LPS-induced TBK1–IKKε–IRF3 axis activation. J Biol Chem 293: 10186-10201.

Turner JR 2009. Intestinal mucosal barrier function in health and disease. Nat Rev Immunol 9: 799-809.

Wang H, Miao F, Ning D, *et al.*, 2022. Ellagic acid Alleviates hepatic ischemia–reperfusion injury in C57 mice via the Caspase-1-GSDMD pathway. BMC Vet Res 18: 229.

Wang X, Wang W, Wang L, *et al.*, 2019a. Lentinan modulates intestinal microbiota and enhances barrier integrity in a piglet model challenged with lipopolysaccharide. Food Funct 10: 479-489.

Wang X, Wang W, Wang L, *et al.*, 2019b. Lentinan modulates intestinal microbiota and enhances barrier integrity in a piglet model challenged with lipopolysaccharide. Food Funct 10: 479-489.

Xu L, Zhao J, Liu M, *et al.*, 2017. A effective DNA vaccine against diverse genotype J infectious hematopoietic necrosis virus strains prevalent in China. Vaccine 35: 2420-2426.

Xu P, Li M, Zhang J *et al.*, 2012. Correlation of intestinal microbiota with overweight and obesity in Kazakh school children. BMC Microbiol 28 (12): 1-6.

Xu X and Zhang X, 2015. Lentinula edodes-derived polysaccharide alters the spatial structure of gut microbiota in mice. PloS One 10: e0115037.

Yang X, Zheng M, Zhou M, *et al.*, 2022a. Lentinan supplementation protects the gut–liver axis and prevents steatohepatitis: The role of gut microbiota involved. Front Nutr 8: 803691.

Yang Y, Song S, Nie Y, *et al.*, 2022b. Lentinan alleviates arsenic-induced hepatotoxicity in mice via downregulation of OX40/IL-17A and activation of Nrf2 signaling. BMC Pharmacol. Toxicol 23: 16.

Yanling W, Jie X, Hao Z, *et al.*, 2023. Qualcomm sequencing analysis of the influence of different wine producing areas in Xinjiang on rat intestinal flora diversity. China Brewing 42.

Yin H, Chai R, Qiu H, *et al.*, 2023. Effects of Isaria cicadae on growth, gut microbiota, and metabolome of Larimichthys crocea. Fish Shellfish Immunol 136: 108719.

Zhang C, Yu M, Yang Y, *et al.*, 2016. Effect of early antibiotic administration on cecal bacterial communities and their metabolic profiles in pigs fed diets with different protein levels. Anaerobe 42: 188-196.

Zhou G, Liu H, Yuan Y, *et al.*, 2024. Lentinan progress in inflammatory diseases and tumor diseases. Sci Total Environ 29: 8.